MO-Theoretical Studies on a Model Complex for Deoxymyoglobin

Christian Kollmar, Sighart F. Fischer, and Michael C. Böhm[a]
Physik Department, Theoretische Physik T38, Technische Universität München,
James Franck Straße, D-85748 Garching
[a] Institut für Physikalische Chemie, Physikalische Chemie III, Technische Universität Darmstadt,
Petersenstraße 20, D-64287 Darmstadt

Z. Naturforsch. **53 a,** 755–765 (1998); received July 1, 1998

The origin of the displacement of the Fe atom in deoxymyoglobin with respect to the porphyrin plane in the high-spin state is examined by a qualitative molecular orbital (MO) analysis on the extended Hückel level. We find that attachment of a fifth ligand (imidazole in our model complex) to Fe(II)porphyrin favors the out-of-plane shift due to a strengthening of the bonding interaction between Fe and the nitrogen of the imidazole ligand. This results in a high-spin ($S = 2$) ground state with Fe shifted out-of-plane for the five-coordinate complex instead of an intermediate spin ground state ($S = 1$) with Fe lying in the plane for four-coordinate Fe(II)porphyrin. The relative energies of the different spin states as a function of the distance between Fe and the porphyrin plane are evaluated using an ROHF (restricted open shell Hartree-Fock) version of an INDO (intermediate neglect of differential overlap) method. We observe a level crossing between high-spin and intermediate spin states whereas the low-spin ($S = 0$) state remains always higher in energy.

Key words: Metalloporphyrines, Electronic Structure, Structural Preferences,
Molecular Orbital Model.

1. Introduction

Tetrapyrrole macrocycles represent an important class of ligands in biological systems due to their ability to bind metal ions thus forming metalloporphyrins. Well-known examples are hemoglobin, myoglobin, chlorophyll, cytochromes and peroxidase which play an important role in the transport, storage and redox reactions of molecular oxygen in organisms. There have been extensive efforts to design model systems which mimic the biological functions of metalloporphyrins [1, 2]. Theoretical studies on the electronic structure of metalloporphyrins and models for the corresponding functional units in biological systems are also abundant [3 - 32]. The electronic structure investigations published in the past three decades cover a range from one-electron models of the extended Hückel (EH) type over semiempirical single- and many-determinantal approaches to ab initio methods. The improved computational efficiency achieved in recent years rendered possible complete active space self-consistent-field (CASSCF) calculations [24, 25] as well as density functional studies coupled to a Car-Parrinello molecular dynamics [30]. Both the CASSCF [24, 25] and earlier semiempirical studies of the many-determinantal type have shown the importance of electron correlation in dioxygen heme complexes. In those systems, a single determinantal wavefunction does not allow a quantitative description of all aspects of the corresponding electronic structure. Inspection of the literature shows that even highly advanced electronic structure calculations still leave open questions in our understanding of electronic structure effects of metalloporphyrins. These have been the main motivation of the present model study which has the intention to demonstrate the utility of simple molecular orbital (MO) concepts in the qualitative understanding of certain bonding properties in metalloporphyrins. Such an approach is of particular interest if it leads to an explanation of experimental observations.

Experimental information on the electronic structure of iron porphyrin complexes and related biological units is obtained from Mössbauer spectroscopy [33 - 36]. The experimentally observed gradients of the electric field at the nuclear site of the iron ion can be fitted using a phenomenological crystal-field

---

Reprint requests to Prof. Dr. Sighart F. Fischer;
FAX: +49 89 2891 2444, Phone: +49 89 2891 2373.

0932–0784 / 98 / 0900–0755 $ 06.00 © Verlag der Zeitschrift für Naturforschung, Tübingen · www.znaturforsch.com

Hamiltonian including spin-orbit coupling [33 - 36]. However, it is sometimes difficult to fit the experimental results by a unique set of model parameters. Moreover, the sensitivity of the Mössbauer spectra to the variation of structural parameters is not always guaranteed. It has been assumed for quite a long time that small displacements of the iron with respect to the porphyrin plane would not significantly affect the electric field gradient at the iron nucleus [12]. Although Mössbauer spectra are a valuable source of information on the electronic structure of iron complexes it remains a difficult task to establish a clear relationship between the experiments and the results of theoretical calculations.

The distance between the iron atom and the plane of the porphyrin unit in myoglobin and hemoglobin is an important structural parameter which determines the ability to bind ligands like CO or O_2. It is generally assumed that the quarternary structure of hemoglobin leads to a cooperative effect induced by the attachment of an O_2 ligand to one of the four heme units. This process triggers a structural transition from the so-called T- to the R-form of the heme, thus facilitating the attachment of additional O_2 ligands to the remaining hemes of the quarternary unit [37]. This increased affinity to oxygen binding is due to a reduction of the distance between the Fe atom and the porphyrin plane accompanying the structural transition from the T- to the R-form.

It is well-known that deoxymyoglobin has a high-spin ($S = 2$) ground state with four unpaired electrons mainly localized on the iron. Even if it is clear that an out-of-plane shift of the Fe atom and the corresponding reduction of the ligand field splitting will favor the high-spin as compared to low-spin and intermediate-spin states, one may raise the question in the first place why the Fe atom moves away from the porphyrin plane in deoxymyoglobin with a five-coordinate Fe atom but not in the four-coordinate Fe(II)porphyrin complex. This displacement has previously been ascribed to a non-bonded interaction between the nitrogen lone pair of the imidazole ligand and the lone pairs of the pyrrole nitrogens of the porphyrin [13]. A quantification of this suggestion, however, has not been given. In the present contribution we would like to reinvestigate this question on the basis of semiempirical MO calculations. Due to the violation of the aufbau principle in these compounds, the application of many standard ab initio Hartree Fock black box programs turned out to be unsuitable. Other highly sophisticated techniques [24, 25, 30] may have the disadvantage that transparent interpretations of computational results are difficult. We therefore decided to focus on qualitative arguments of the same type as those used by Hoffmann and coworkers [38, 39] in their transparent analyses of transition metal compounds. Such arguments do not depend on the details of the corresponding computational tool. Thus, the following analysis relies exclusively on MO calculations of the extended Hückel type [38] and a restricted open shell Hartree-Fock (ROHF) version [40] of an intermediate neglect of differential overlap (INDO) Hamiltonian developed for transition metal compounds [41]. Although the present strategy does not lead to results of quantitative accuracy we would like to demonstrate the utility of qualitative concepts for our understanding of the electronic structure of metalloporphyrins. Instead of presenting "exact" numbers we evaluate a general interaction mechanism which is controlled by the symmetry of the atomic orbitals and electronic occupation numbers.

The organization of the present contribution is as follows. In Sect. 2 we describe the results of extended Hückel calculations on a model for deoxymyoglobin. In Sect. 3 the relative energies of the different spin states are analyzed as a function of the distance between Fe and the porphyrin plane using the aforementioned ROHF version [40] of the INDO method of [41]. The article ends with a short resume. The computational conditions of the EH calculations as well as an energy fragmentation within the EH formalism are given in an appendix.

2. Extended Hückel Calculations on a Model for Deoxymyoglobin

Our deoxymyoglobin model is shown in Figure 1. The terminal groups of the heme have been replaced by hydrogens and the proximal histidine by imidazole for which we assume the geometry of the free molecule [42]. The distances between the center of the porphyrin ring and each of the four pyrrole nitrogens and between Fe and the nitrogen of imidazole are taken as 1.97 and 2.1 Å, respectively. Note that the Fe atom is not necessarily located in the porphyrin plane. This topic is the central subject of the following analysis. The coordinate system with its origin in the center of the porphyrin ring has been chosen such that the z axis is perpendicular to the porphyrin plane and

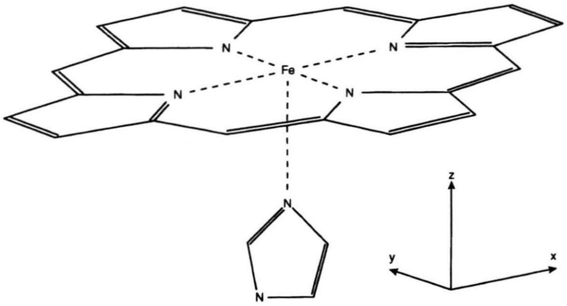

Fig. 1. Schematic representation of the deoxymyoglobin model complex. The *xy*-plane corresponds to the porphyrin plane with the four nitrogens being located on the *x* and *y* axes. The imidazole ligand lies in the *xz* plane. The hydrogen atoms have been omitted in the simplified diagram. In the schematic display Fe is located in the porphyrin plane.

that the four pyrrole nitrogens lie on the *x* and *y* axes. The imidazole ring is assumed to lie in the *xz*-plane thus eclipsing two Fe-N bonds as suggested by X-ray structure data for deoxymyoglobin [43].

We already mentioned the out-of-plane displacement of Fe in the five-coordinate complex denoted as ImFe(II)P in the following and shown schematically in Figure 1. This displacement, which is not shown in Fig. 1, leads to a high-spin ground state ($S = 2$). The four-coordinate complex Fe(II)porphyrin Fe(II)P, on the other hand, has an intermediate-spin ground state ($S = 1$) with the iron located in the porphyrin plane. One may therefore assume that the fifth ligand plays an essential role for the out-of-plane shift of Fe. It is illustrative to consider the change in the total energy of the complex in the high-spin state as a function of the distance d_{Fe-P} between the metal and the porphyrin plane for both the five-coordinate model complex ImFe(II)P and four-coordinate Fe(II)P as obtained from extended Hückel calculations. The EH papameters employed are summarized in the appendix. On variation of d_{Fe-P} we always keep the distance between Fe and the nitrogen of imidazole at a fixed value of 2.1 Å, i.e., we move the subunit Fe-imidazole as a whole. The results of the extended Hückel calculations are shown in Figure 2. The Fe 3d orbital occupation for the high-spin state is $(d_{xy})^2(d_{xz})^1(d_{yz})^1(d_{z^2})^1(d_{x^2-y^2})^1$ (see below). Although the extended Hückel method cannot be expected to provide quantitative results with respect to variation of geometry parameters the qualitative shape of the curves is interesting. It can be seen that the position of Fe at the energy minimum is outside the porphyrin plane in both cases. However, we observe only a very shallow minimum for Fe(II)P, whereas the minimum for ImFe(II)P is much more pronounced indicating that the presence of the fifth ligand favors the out-of-plane displacement of Fe. The extended Hückel calculations for the triplet states of both the four- and five-coordinate complexes (not shown here) yield an equilibrium position of the iron in the porphyrin plane. We will elucidate these structural features on the basis of a qualitative MO analysis in the following.

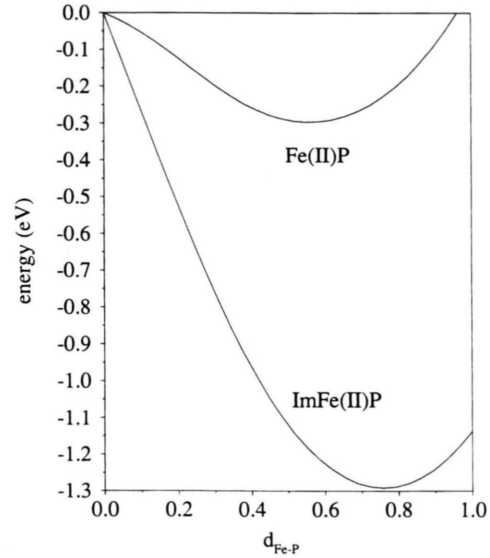

Fig. 2. Energy of the high-spin state as a function of the distance d_{Fe-P} (in Å) for the four-coordinate Fe(II)P and the five-coordinate ImFe(II)P complex. The numerical results have been obtained from extended Hückel calculations. The energy obtained for Fe lying in the porphyrin plane has been chosen as the zero point of the energy scale in both cases.

Let us first consider the interaction between Fe and the four N atoms of the porphyrin ligand. The symmetry-adapted linear combinations of the N lone-pair orbitals which act as σ donors to the metal are given in Scheme 1. The labels of the irreducible representations refer to the symmetry group D_{4h} of the four-coordinate complex. π-backbonding from the metal

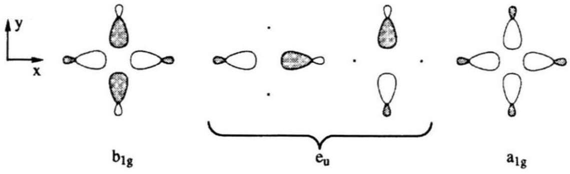

Scheme 1.

to the pyrrole nitrogens plays only a minor role and will not be considered here. The metal-ligand bonding is largely determined by the overlap between the N lone pair orbitals given in Scheme 1 and Fe atomic orbitals (AO's) of the same symmetry, i. e., $b_{1g} - 3d_{x^2-y^2}$, e_u – $4p_x$, $4p_y$ and a_{1g} – $3d_{z^2}$, 4s. The interaction between these ligand and Fe orbitals leads to bonding linear combinations with predominant ligand character which are all doubly occupied. It should be noted that this interpretation is somewhat simplified because the bonding interaction may be spread out over several ligand MO's rather than being concentrated within a single ligand MO for each symmetry. Such a simple two-orbital picture defined by a bonding-antibonding pair provides, however, a convenient short-hand interpretation of the metal-ligand interaction. Of course, the antibonding MO's of this metal-ligand coupling exhibit pedominant metal character. However, with one exception for the high-spin state, these antibonding MO's are not occupied as we will see shortly.

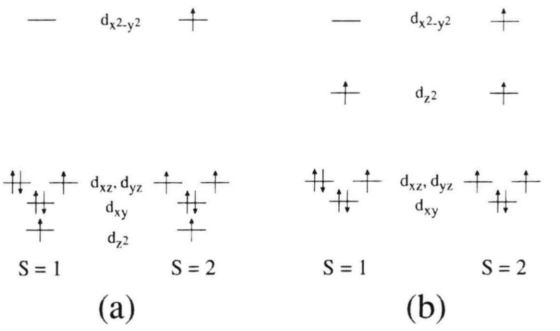

Fig. 3. Schematic MO energy splitting of the orbitals with predominant metal 3d character for the four-coordinate Fe(II)P complex (a) and the five-coordinate model complex ImFe(II)P (b). The orbital occupancies are shown for an intermediate-spin ($S = 1$) and a high-spin ($S = 2$) state.

To get an idea of the orbital occupation in the different spin states we have to consider the ligand field splitting of the orbitals with predominant metal 3d character as represented schematically in Figure 3. In four-coordinate Fe(II)P (Fig. 3(a)) there are four MO's (d_{xy}, d_{xz}, d_{yz}, d_{z^2}) which show only little mixing with ligand orbitals. These MO's remain almost pure metal orbitals and are close in energy; lower set of MO's. The Fe $3d_{x^2-y^2}$ AO, on the other hand, has a favorable overlap with the linear combination of N lone pair orbitals of b_{1g} symmetry shown in Scheme 1 thus interacting more strongly with this symmetry-adapted ligand orbital. This results in an energetic up-shift of the antibonding component of this interaction. Thus, the MO derived from $d_{x^2-y^2}$ is just one of the aforementioned antibonding MO's with predominant metal character. In the following we will always denote MO's with predominant metal 3d character by the corresponding AO labels.

If we attach the fifth ligand, i. e., imidazole in our model complex, the $3d_{z^2}$ orbital finds also a partner to interact with because it overlaps favorably with the lone-pair orbital of the pyridine-like nitrogen of imidazole. The antibonding MO resulting from this coupling is denoted as d_{z^2} in Figure 3b). Its destabilization is, however, less pronounced than that of $d_{x^2-y^2}$ (see Figure 3b)). This is mainly due to a hybridization with Fe 4s and $4p_z$ orbitals which attenuates the antibonding interaction (see below).

The Fe 3d orbital occupations used in our calculations are also given in Figure 3. In the case of the five-coordinate complex ImFe(II)P (Fig. 3b) we take the occupation of the ground state for each spin multiplicity as obtained from the INDO calculations described below. Please note that configurations generated via a redistribution of the spins in the MO's d_{xy}, d_{xz}, d_{yz} are very close in energy. Fortunately, it turned out that the occupation of the low-lying MO's d_{xy}, d_{xz}, d_{yz} is not relevant for the following considerations. Since there are mainly the MO's d_{z^2} and $d_{x^2-y^2}$ within the 3d orbital block which are strongly involved in metal ligand bonding all what matters in the present context is the occupation of these two orbitals. This insensitivity of the results has been checked by INDO calculations for other orbital populations within the d_{xy}, d_{xz}, d_{yz} orbital set. In other words, in the present work we discuss a problem in the language of simple MO arguments although the exact orbital occupation of the ground state cannot be determined within this degree of sophistication. This point has been touched upon already in the introduction. The MO d_{z^2} is always singly occupied whereas $d_{x^2-y^2}$ is empty in the intermediate-spin and singly occupied in the high-spin state. In the case of Fe(II)P (Fig. 3a) we use the same orbital occupations as for the five-coordinate complex for reasons of comparability even if these do not correspond to the ground state.

After having described some of the basic features of metal-ligand interaction and the corresponding ligand-field splitting of the metal 3d orbitals in both Fe(II)P and ImFe(II)P, we would like to investigate how these properties are influenced by a variation

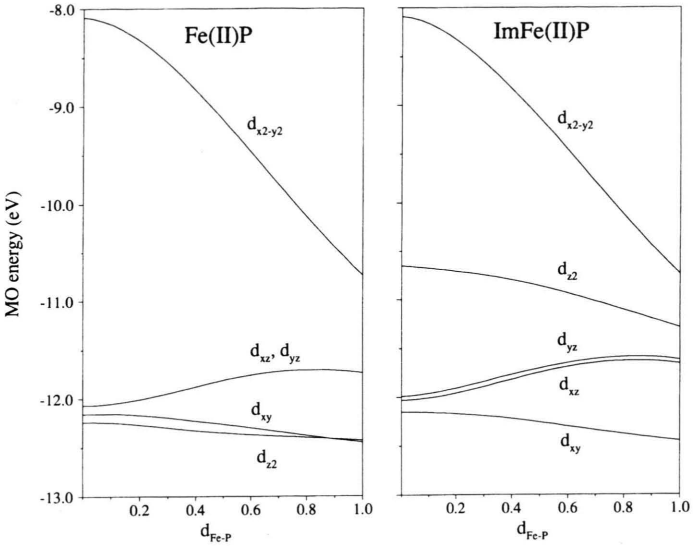

Fig. 4. Energies ε_i of the MO's with predominant metal 3d character as a function of the distance $d_{\text{Fe-P}}$ (in Å) for the four-coordinate Fe(II)P and the five-coordinate ImFe(II)P complex. The numerical results have been obtained from extended Hückel calculations.

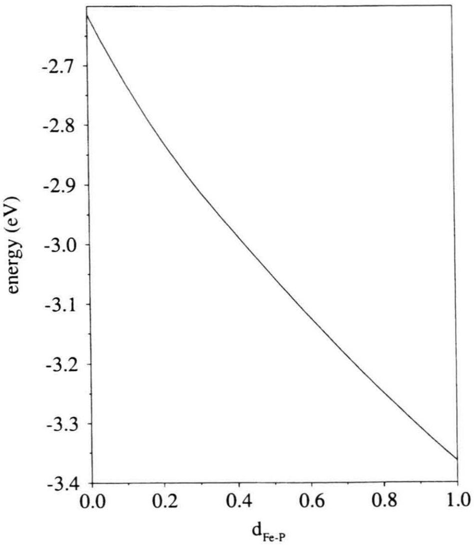

Fig. 5. Two-center bond energy $E_{\text{Fe-N}}$ between Fe and the neighboring N atom of imidazole as a function of the distance $d_{\text{Fe-P}}$ (in Å). The numerical results have been obtained from extended Hückel calculations.

of the distance $d_{\text{Fe-P}}$. It is obvious that an out-of-plane displacement of the iron reduces all overlaps which favor metal-ligand bonding between Fe and porphyrin even if the lowering of the symmtery from D_{4h} to C_{4v} allows additional $\sigma - \pi$ mixing. Thus, the bonding interaction between Fe and the N atoms of porphyrin is expected to be weakened. However, since the Fe-N(porphyrin) antibonding $d_{x^2-y^2}$ orbital is empty in the intermediate-spin state but singly occupied in the high-spin state, the metal-ligand bonding between Fe and porphyrin and the loss of this bonding resulting from the displacement of Fe is much more pronounced for the former than for the latter. It is therefore not surprising that the energy minimum of the intermediate-spin state is obtained for Fe lying in the plane, whereas the balance of metal-ligand interactions as a function of the distance $d_{\text{Fe-P}}$ is less obvious for the high-spin state.

The extended Hückel MO energies ε_i of orbitals with predominant metal 3d character as a function of the distance $d_{\text{Fe-P}}$ are shown in Fig. 4 for both Fe(II)P and ImFe(II)P. First, it should be noted that these energies do not differ significantly for the two compounds except for d_{z^2}. In both systems, it is the MO $d_{x^2-y^2}$ which undergoes the most dramatic change as a function of the out-of-plane shift. It looses much of its antibonding character as a consequence of the decreased overlap between $d_{x^2-y^2}$ and the symmetry-adapted b_{1g} linear combination of lone pair orbitals (see Scheme 1). Of course, the corresponding bonding interaction which can be retrieved in lower-lying MO's with predominant ligand character is also reduced resulting in an energetic up-shift of these orbitals (not shown here). In the high-spin state, this up-shift of the doubly occupied MO's is compensated to a large extent by the down-shift of the singly occupied $d_{x^2-y^2}$ MO such that the net effect of the Fe displacement on bonding between Fe and the porphyrin ligand MO is much smaller than for the intermediate-spin state.

The principal difference between the two compounds is given by the energetic position of the d_{z^2} orbital. It is this orbital that must be analyzed in some more detail if we want to understand the pronounced out-of-plane energy minimum of the high-spin state of ImFe(II)P. It can be seen from Fig. 4 that this orbital is considerably higher in energy in the five-coordinate as compared to the four-coordinate complex. The diagram shows that the energy of d_{z^2} as a function of $d_{\text{Fe-P}}$ changes very little for Fe(II)P whereas one observes a considerable down-shift for ImFe(II)P. This is somewhat surprising given the fact that this orbital

Table 1. Metal AO coefficients of the MO with predominant $3d_{z^2}$ character obtained from extended Hückel calculations as a function of the distance d_{Fe-P}.

d_{Fe-P}	$3d_{z^2}$	4s	$4p_z$
0.0	0.81	0.16	0.21
0.2	0.81	0.13	0.19
0.4	0.80	0.08	0.18
0.6	0.79	0.03	0.16
0.8	0.78	–0.02	0.14

interacts mainly with the N lone pair orbital of imidazole. Remember that the distance between Fe and imidazole remains fixed.

The energetic down-shift of d_{z^2} in ImFe(II)P might be explained by a weakening of the antibonding interaction between Fe and N(imidazole) for this orbital. A reduction of the antibonding interaction should strengthen the bond between these atoms. To confirm this hypothesis it will be useful to calculate the diatomic interaction energy of the corresponding metal-ligand atom pair. The definition of such a diatomic bond energy E_{AB} between two atoms A and B is given in the appendix. Using Eq. (9), the bond energy between Fe and the nitrogen of imidazole as a function of the distance d_{Fe-P} is shown in Figure 5. It can be seen that there is a considerable strengthening of the Fe-N(imidazole) bonding interaction with increasing d_{Fe-P} in the five-coordinate complex.

We have already mentioned the important role of the the MO with predominant $3d_{z^2}$ character. Thus, we would like to analyze this MO in some more detail. The first order admixture of the σ donating N lone pair orbitals denoted as σ_P and σ_{Im} for porphyrin and imidazole, respectively, to this MO is antibonding for both ligands. Apart from this dominant mixing, the MO $3d_{z^2}$ is also slightly hybridized with contributions from Fe 4s and $4p_z$. The coefficients for the Fe $3d_{z^2}$, 4s and 4p AO's of this MO as a function of the distance d_{Fe-P} are given in Table 1. It can be seen that the $3d_{z^2}$ contribution remains almost constant. Whereas the hybridization with $4p_z$ does not change very much, we observe a more pronounced change of the hybridization with 4s on variation of the distance d_{Fe-P}. In terms of perturbation theory, the admixture of 4s to $3d_{z^2}$ may be classified as a second order effect [44] occuring via interactions with N lone pair orbitals of the porphyrin or the imidazole ligand. The relevant Fe and ligand orbitals are shown schematically in Scheme 2. This second order effect modifies the antibonding interaction between Fe and the imidazole ligand. The sign and thus the energetic influence of the second order admixture $c_{4s,3d_{z^2}}$ of 4s to $3d_{z^2}$ can be extracted from the following expression [44] which is based on conventional perturbation theory:

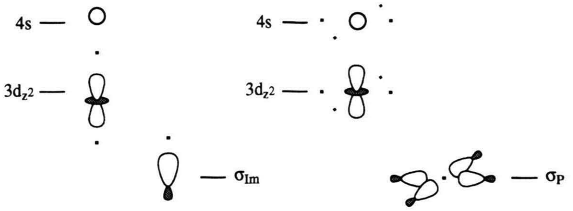

Scheme 2.

$$c_{4s,3d_{z^2}} \sim \frac{S_{3d_{z^2}-\sigma} S_{\sigma-4s}}{(\varepsilon_{3d_{z^2}} - \varepsilon_{4s})(\varepsilon_{3d_{z^2}} - \varepsilon_{\sigma})}.$$

The two elements in the numerator denote overlap integrals $S_{3d_{z^2}-\sigma}$ or $S_{\sigma-4s}$ between nitrogen lone pair orbitals (σ) and, respectively, Fe $3d_{z^2}$ or 4s AO's. The denominator of this expression contains differences between the MO energy levels shown in Scheme 2. It is easily verified that it is negative for both σ_P and σ_{Im}. The product of overlap integrals in the numerator, however, is positive for σ_{Im} but negative for σ_P ($S_{3d_{z^2}-\sigma_{Im}} > 0$, $S_{3d_{z^2}-\sigma_P} < 0$). This is a consequence of the negative lobe of the $3d_{z^2}$ AO in the *xy*-plane. Hence, the two second order mixings of 4s with $3d_{z^2}$ are of opposite sign depending on whether they occur via the porphyrin or via the imidazole ligand. In the latter case, the Fe 4s contribution to $3d_{z^2}$ has a negative sign like the first order contribution σ_{Im} so that 4s and σ_{Im} interfere in a bonding fashion thus weakening the overall antibonding interaction between Fe and imidazole in the MO with predominant $3d_{z^2}$ character. The opposite effect is observed for the second order mixing of 4s with $3d_{z^2}$ via the porphyrin ligand which enhances the antibonding interaction between Fe and imidazole for the MO $3d_{z^2}$. An increase of the distance d_{Fe-P} lowers the overlap integral between σ_P and $3d_{z^2}$ but leaves the overlap integral between σ_{Im} and $3d_{z^2}$ unchanged. The weight of the second order mixing via the porphyrin ligand is therefore diminished which weakens the antibonding interaction between Fe and N(imidazole) for the MO $3d_{z^2}$. It should be noted that our explanation of the rehybridization of the $3d_{z^2}$ MO with 4s is still somewhat oversimplified because the overlap between the p_z orbitals of N(porphyrin) and $3d_{z^2}$ increases from zero to finite values as the iron is moved out of the plane. This additional mixing even enhances the rehybridization described above.

3. Relative Energies of the Different Spin States, Charge and Spin Distributions

In the preceding section we tried to explain how the attachment of a fifth ligand to Fe(II)porphyrin favors the out-of-plane shift of Fe in the high-spin state. The corresponding considerations are not relevant for the position of Fe in the intermediate-spin state because in this case the weakening of the bonding interaction between Fe and porphyrin resulting from the out-of-plane shift overrides all other effects. Even if the transparency of the extended Hückel method is helpful in a qualitative analysis of the metal-ligand bonding this approach does not give any information on the relative stabilities of different spin states because it does not take into account the exchange stabilization of the high-spin state. The preceding considerations rest on the assumption that the high-spin state of ImFe(II)P is really the ground state for the distance $d_{\mathrm{Fe-P}}$ where the energy hyperface of the high-spin state exhibits a minimum. To clarify this point it is useful to calculate the relative energies of the different spin states as a function of the distance $d_{\mathrm{Fe-P}}$. This will be done using a ROHF version of an INDO method developed for transition metal compounds [41]. It should be noted at the outset that this method does not provide energy curves of trustworthy accuracy as a function of geometry parameters like the distance $d_{\mathrm{Fe-P}}$. For example, one does not obtain an out-of-plane energy minimum for the high-spin state. One might also have doubts about the accuracy of semiempirical one-determinantal results for relatively small energy gaps between different spin multiplets. However, it turns out that at least the qualitative behavior of these energy gaps looks reasonable even if the calculated numbers should perhaps not be taken too literally. The INDO model of [41] has already been employed in the study of the energetic splitting of spin multiplets in transition metal complexes [45].

The states to be considered in the following correspond to the configurations shown in Figure 3. The Fe 3d occupation of the high-spin state reads $(d_{xy})^2(d_{xz})^1(d_{yz})^1(d_{z^2})^1(d_{x^2-y^2})^1$. The intermediate spin state is given by $(d_{xy})^2(d_{xz})^2(d_{yz})^1(d_{z^2})^1$ (^{3}A") or $(d_{xy})^2(d_{xz})^1(d_{yz})^2(d_{z^2})^1$ (^{3}A') for ImFe(II)P. This spin configuration differs from that of Fe(II)P given by $(d_{xy})^2(d_{xz})^{1.5}(d_{yz})^{1.5}(d_{z^2})^1$ in a degenerate ^3E_g state. Although attachment of the imidazole ligand lowers the symmetry from C_{4v} to C_s the two states ^{3}A" and ^{3}A' remain approximately degenerate. In addition, we also consider the singlet state $(d_{xy})^2(d_{xz})^2(d_{yz})^2$.

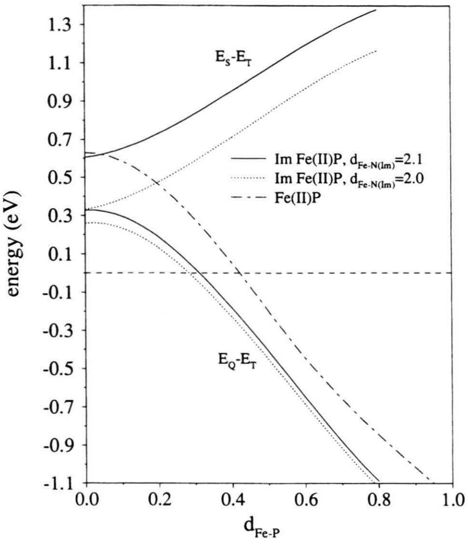

Fig. 6. Energies of the low-spin (E_S) and the high-spin state (E_Q) relative to the intermediate-spin state (E_T) as a function of the distance $d_{\mathrm{Fe-P}}$ (in Å) for the five-coordinate model complex ImFe(II)P with the distance Fe-N(imidazole) being 2.1 Å (full line) or 2.0 Å (dotted line). The energy gap $E_Q - E_T$ for Fe(II)P is also shown. The numerical results have been obtained from INDO calculations.

The relative energies of these states as a function of the distance $d_{\mathrm{Fe-P}}$ are shown in Fig. 6 by the full lines for our model complex of deoxymyoglobin. It can be seen that the low-spin state is of no particular interest because its energy is always higher than the energies of both the intermediate- and the high-spin state. For the iron lying in the porphyrin plane we obtain an intermediate-spin ground state as for Fe(II)porphyrin. The out-of-plane displacement of Fe clearly favors the high-spin state so that one observes a level crossing at a distance of ~ 0.3 Å with the high-spin state being the ground state for larger distances. Given the fact that the distance between Fe and the porphyrin plane amounts to ~ 0.4 Å in deoxymyoglobin [43], this seems reasonable.

The energetic splitting in Fig. 6 is at variance with those obtained from a Mössbauer fit using a crystal-field Hamiltonian [33 - 36]. These latter calculations place the low-spin state in between the high-spin ground state and the intermediate-spin state. In our

Table 2. Net charges on Fe, porphyrin (P) and imidazole (Im) for the different spin states as obtained from INDO calculations. In the case of the intermediate-spin state we give the numbers for $^3A'$. The numbers of $^3A''$, however, are almost identical, differing by 0.001 electron charges at the most.

d_{Fe-P}	$S = 2$			$S = 1$			$S = 0$		
	Fe	P	Im	Fe	P	Im	Fe	P	Im
0.0	1.097	−1.250	0.153	0.815	−0.924	0.109	0.688	−0.914	0.226
0.8	1.006	−1.125	0.118	0.803	−0.903	0.100	0.709	−0.906	0.197

Table 3. Spin densities on Fe, porphyrin (P) and imidazole (Im) for the high-spin and intermediate-spin states (in %) as obtained from INDO calculations. In the case of the intermediate-spin state we give the numbers for $^3A'$. The numbers of $^3A''$ are again almost identical.

d_{Fe-P}	$S = 2$			$S = 1$		
	Fe	P	Im	Fe	P	Im
0.0	81.8 %	14.9 %	3.3 %	90.9 %	4.6 %	4.5 %
0.8	80.1 %	18.0 %	1.9 %	91.9 %	5.0 %	3.1 %

calculations, the low-spin state remains the energetically highest state even for $d_{Fe-P} = 0$ where the probability for a low-spin ground state should be highest. We do not know whether or not this is an artifact of the INDO parametrization adopted. It is clear that the energetic position of the low-spin state relative to the other multiplets is most strongly influenced by the energy of the $3d_{z^2}$ MO, i. e., by the interaction with the axial ligands. Attachment of a sixth ligand like CO leads to an energetic up-shift of $3d_{z^2}$ resulting in a low-spin ground state. Shortening the distance between Fe and imidazole should also enhance the axial interaction thus raising the energy of the $3d_{z^2}$ MO. The energy gaps for a reduced distance of 2.0 Å between Fe and N(imidazole) are therefore also shown in Fig. 6 (broken line). It turns out that this shortening is not sufficient to change the energetic sequence of the multiplets although it lowers the energy of the low-spin state relative to the intermediate- and high-spin states.

It is interesting to compare the energy splittings between the high-spin and intermediate-spin states for ImFe(II)P and Fe(II)P. The energy splitting of the latter is therefore also shown in Fig. 6 as a function of d_{Fe-P}. It can be seen that the energy of the high-spin relative to the intermediate-spin state is always higher for Fe(II)P than for ImFe(II)P. Consequently, the crossing point from an intermediate- to a high-spin ground state is shifted to larger distances (> 0.4 Å) for Fe(II)P. Thus, the high-spin state is favored in ImFe(II)P as compared to Fe(II)P no matter if the Fe atom is located in or outside the porphyrin plane. Apart from the arguments presented in the previous section, the decreased high-spin-intermediate-spin energy gap in ImFe(II)P also contributes to shifting the energy minimum of the high-spin state (Fe out of plane) below the energy minimum of the intermediate-spin state (Fe in plane).

The net charges of Fe and the porphyrin and imidazole ligands are given in Table 2 for $d_{Fe-P} = 0$ and 0.8 Å. It can be seen that the out-of-plane shift of Fe does not lead to a significant change of the charge distribution. The positive charge on Fe is highest for the high-spin state and decreases with decreasing spin multiplicity. This is in agreement with expectation. Comparing the d orbital occupation of the triplet state to that of the singlet, we note that one electron is shifted from a doubly occupied MO with predominant metal character (either d_{xz} or d_{yz}) to d_{z^2} which has a sizeable admixture from the lone pair orbital of N(imidazole). Thus, one would expect a shift of electron density from Fe to imidazole. This is confirmed by the numbers in Table 2 indicating a shift of ~ 0.1 electron charges. Going from the triplet to the quintet state, yet another electron is shifted from the remaining doubly occupied orbital of the d_{xz}, d_{yz} orbital pair to $d_{x^2-y^2}$ which has a significant contribution from the porphyrin ligand. Thus, the shift of electron density occurs now mainly from Fe to porphyrin making the former more positive and the latter more negative by ~ 0.3 electron charges.

The distribution of the spin density on Fe, porphyrin and imidazole is shown in Table 3. Again there is only a minor influence of the Fe position on the computational results. In the case of the triplet, the spin density is mainly concentrated on the iron with the remaining 10% being roughly equally distributed on the porphyrin and imidazole ligands. For the quintet state, we observe an enhanced spin density of ~ 15% on the porphyrin. This is due to the occupation of the $d_{x^2-y^2}$ MO which exhibits a considerable mixing with the symmetry-adapted linear combination of the N lone pair orbitals of the porphyrin (b_{1g} in Scheme 1). It should be noted that the spin density on the ligands is almost exclusively localized on the N atoms adjacent to Fe.

4. Conclusions

In the present investigation we developed a qualitative picture focussing on the influence of the ligand environment on the position of Fe relative to the porphyrin plane in deoxymyoglobin. Even if variation of the distance $d_{\mathrm{Fe-P}}$ influences the MO's in several ways it is possible to single out a dominant effect with respect to the modification of the bonding interaction between Fe and the nitrogen of imidazole. It turned out that the strengthening of this bond is responsible for the out-of-plane shift of Fe which has been observed in X-ray investigations. To a large extent, it is due to a rehybridization of the MO with predominant $3d_{z^2}$ character. In order to explain the structural observations it is not necessary to suggest any interaction between nitrogen lone pairs of both ligands. We wish to reemphasize that we are aware of the qualitative character of our model. Nevertheless, we think that our arguments are still valid if we take into account that the environment in realistic heme systems is more complex than that of our simple model system.

In our model, the only variable geometry parameter is the distance between the iron and the porphyrin plane, whereas the distance between Fe and imidazole remains fixed. However, if the out-of-plane shift of Fe strengthens the bond between Fe and N(imidazole) it is clear that the corresponding bond distance must be shortened. Thus, there is a coordinated motion of Fe and the imidazole ligand, i. e., the distance Fe-N(imidazole) is shortened if the distance $d_{\mathrm{Fe-P}}$ gets larger, and vice versa. Although the whole complex is embedded into a protein environment of great complexity, such a coordinated motion might explain how the position of Fe relative to the heme plane can be modified by structural changes in the environment. The imidazole ligand is just the terminal group of a large histidine residue. Structural modifications pushing this ligand towards the porphyrin or pulling it away from it would, respectively, increase or decrease the distance $d_{\mathrm{Fe-P}}$. This is in perfect agreement with the results of Mössbauer fits which give a significantly larger axial ligand field splitting for deoxygenated human hemoglobin [35] than for deoxygenated sperm whale myoglobin [33]. Thus, the distance between Fe and imidazole must be shorter in deoxygenated hemoglobin (tense structure, large $d_{\mathrm{Fe-P}}$) than in deoxygenated myoglobin (relaxed structure, smaller $d_{\mathrm{Fe-P}}$) in accordance with a model given by Braunitzer et al. [46]. This observation shows that the present study provides a theoretical concept which can be transferred to larger classes of metalloporphyrines.

Although the MO methods applied in this work are not sufficient to provide reliable energy curves as a function of the distance between Fe and the porphyrin plane, they might give us at least some idea on the shape of these curves and how they differ for four-coordinate Fe(II)P and the five-coordinate model complex ImFe(II)P. The curves in Fig. 2 suggest the possibility that the quintet state with the out-of-plane energy minimum is lower in energy than the triplet state with an in-plane energy minimum for the five-coordinate complex, whereas the reverse holds for the four-coordinate complex. The bond between Fe and the porphyrin ligand is strong in the intermediate-spin state because the Fe-N(porphyrin) antibonding MO with predominant $3d_{x^2-y^2}$ character is not occupied in this case. Thus, we are left with a bonding interaction between the ligand orbitals shown in Scheme 1 and Fe orbitals of the corresponding symmetry. The overlap between these orbitals is considerably weakened if the Fe atom is moved out-of-plane so that we expect an in-plane energy minimum for both Fe(II)P and ImFe(II)P. Since the MO $3d_{z^2}$ is occupied in both the intermediate-spin and the high-spin state, the arguments given above on rehybridization of this MO also apply to the former. In contrast to the high-spin state, however, this rehybridization will not change the qualitative shape of the energy curve in the five-coordinate complex as compared to the four-coordinate one. The strengthening of the bond between Fe and N(imidazole) might just make the energy curve look more flat for the former. The optimum position of Fe in the high-spin state, on the other hand, is not obtained so easily. Due to the much weaker bond between Fe and N(porphyrin) there is a more delicate balance of the different Fe-ligand interactions. Here the second order rehybridization of the MO $3d_{z^2}$ responsible for the strengthening of the bond between Fe and N(imidazole) influences the qualitative shape of the energy curve. It leads to a pronounced out-of-plane energy minimum for the five-coordinate complex whereas the energy curve for the four-coordinate complex is very shallow with the exact position of the minimum being unclear. These ideas are summarized in the qualitative energy curves shown in Figure 7. The shape of the energy curves for the high-spin state corresponds to those shown in Figure 2. The shape of the intermediate-spin curves reflects the following features: (a) the minimum is located at $d_{\mathrm{Fe-P}} = 0$, (b) the curve should be more flat for ImFe(II)P than

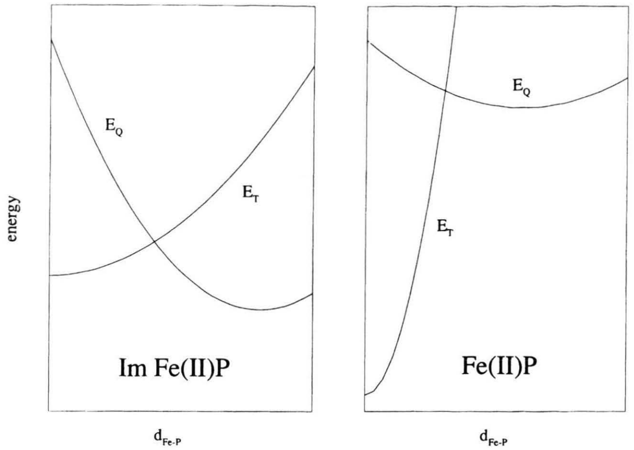

Fig. 7. Qualitative energy curves of the intermediate-spin (E_T) and the high-spin state (E_Q) for ImFe(II)P and Fe(II)P as a function of the distance d_{Fe-P}.

for Fe(II)P and (c) the gap $E_Q - E_T$ between high-spin and intermediate-spin states is larger for Fe(II)P than for ImFe(II)P (see Figure 6). Although more refined methods are needed to obtain accurate electronic energies, we hope to have grasped some important factors governing the position of Fe in this kind of complexes.

Acknowledgements

The present work has been supported by the Fonds der Chemischen Industrie (MCB). We would also like to thank C. Saal who performed ab initio calculations on the deoxymyoglobin model complex using the GAUSSIAN program package and F. Parak for stimulating discussions.

Appendix

The extended Hückel parameters adopted in the present work are given in Table 4.

In the following, a definition of the two-center bond energy E_{AB} between two atoms A and B in the extended Hückel method will be introduced. In this approach, the total energy is just given by the sum of the energies of the occupied orbitals:

$$E = \sum_i n_i \varepsilon_i. \tag{1}$$

ε_i and n_i are, respectively, the energy and the occupation number of the molecular orbital (MO) ψ_i. Representing the MO's as linear combinations of atomic orbitals (AO's) ϕ_r:

$$\psi_i = \sum_r \phi_r C_{ri}, \tag{2}$$

Table 4. Extended Hückel parameters. The coefficients for the double zeta expansion of the Fe 3d orbitals are given in parantheses. Standard extended Hückel parameters have been used for the elements C, N and H.

Element	AO	h_{ii} (eV)	Slater exponent
C	2s	−21.4	1.625
	2p	−11.4	1.625
N	2s	−26.0	1.950
	2p	−13.4	1.950
H	1s	−13.6	1.300
Fe [47]	3d	−12.6	5.35 (0.551) 2.0 (0.626)
	4s	−9.1	1.675
	4p	−5.32	1.100

we may rewrite the total energy as

$$E = \sum_r \sum_s P_{rs} h_{sr} \tag{3}$$

with

$$P_{rs} = \sum_i n_i C_{ri} C_{si}, \tag{4}$$

and h_{rs} being an element of the extended Hückel matrix:

$$\begin{aligned} h_{rs} &= \alpha_r \delta_{rs};\ r, s \in A, \\ h_{rs} &= \frac{1}{2} k(\alpha_r + \alpha_s) S_{rs};\ r \in A, s \in B, A \neq B. \end{aligned} \tag{5}$$

S_{rs} is the overlap integral between the AO's ϕ_r and ϕ_s. k = 1.75 is the Wolfsberg-Helmholtz constant. Using (5) the total energy may again be rewritten:

$$E = \sum_r N_r \alpha_r + \sum_{r \neq} \sum_s P_{rs} \beta_{sr}, \tag{6}$$

where we have introduced the AO occupation number

$$N_r = \sum_s P_{rs} S_{sr} \tag{7}$$

and the resonance integral

$$\beta_{rs} = \frac{1}{2}(k-1)(\alpha_r + \alpha_s)S_{rs}. \tag{8}$$

Note that N_r corresponds to the electronic charge in AO ϕ_r as obtained by a Mulliken population analysis [48]. The first term on the right hand side of (6) consists of "atomic energy levels" α_r multiplied by the corresponding orbital occupation number and represents the energy of the separated atoms in this simple model. The bonding energy of the composite system is given by the second term on the right hand side of (6) and it is this expression we would like to use for a definition of the bond energy between two atoms A and B:

$$E_{AB} = 2\sum_{r\in A}\sum_{s\in B} P_{rs}\beta_{sr}. \tag{9}$$

The bond energies calculated above are obtained from (9).

[1] The Porphyrins, Vol. I-VII, D. Dolphin (ed.), Academic Press, New York 1978, 1979.
[2] Structure Bonding (Berlin), J. W. Buchler (ed.), **64**, 1 (1987).
[3] M. Zerner and M. Gouterman, Theor. Chim. Acta **4**, 44 (1966).
[4] M. Zerner and M. Gouterman, Theor. Chim. Acta **6**, 363 (1966).
[5] W. R. Scheidt, M. Gouterman, in: Iron Porphyrins, A. B. P. Lever and H. B. Gray (eds.), Addison-Wesley, Reading, Massachusetts 1983.
[6] W. D. Edwards, B. Weiner, and M. C. Zerner, J. Amer. Chem. Soc. **108**, 2196 (1986).
[7] G. H. Loew and R. F. Kirchner, Biophys. J. **22**, 179 (1978).
[8] R. F. Kirchner and G. H. Loew, J. Amer. Chem. Soc.**99**, 4639 (1977).
[9] G. H. Loew and R. F. Kirchner, Int. J. Quant. Chem. Quant. Biology Symp. **5**, 403 (1978).
[10] Z. S. Herman and G. H. Loew, J. Amer. Chem. Soc. **102**, 1815 (1980).
[11] Z. S. Herman, G. H. Loew, and M.-M. Rohmer, Int. J. Quant. Chem. Quant. Biology Symp. **7**, 137 (1980).
[12] G. H. Loew, in: Iron Porphyrins, A. B. P. Lever and H. B. Gray (eds.), Addison-Wesley, Reading, Massachusetts 1983.
[13] B. D. Olafson and W. A. Goddard III, Proc. Natl. Acad. Sci. USA **74**, 1315 (1977).
[14] M.-M. Rohmer, A. Dedieu, and A. Veillard, Theor. Chim. Acta **39**, 189 (1975).
[15] A. Dedieu, M.-M. Rohmer, and A. Veillard, J. Amer. Chem. Soc. **98**, 5789 (1976).
[16] A. Dedieu, M.-M. Rohmer, H. Veillard, and A. Veillard, Nouv. J. Chim. **3**, 653 (1979).
[17] A. Dedieu, M.-M. Rohmer, and A. Veillard, Adv. Quant. Chem. **16**, 43 (1982).
[18] H. Kashiwagi and S. Obara, Int. J. Quant. Chem. **20**, 843 (1981).
[19] S. Obara and H. Kashiwagi, J. Chem. Phys. **77**, 3155 (1982).
[20] S. F. Sontum and D. A. Case, J. Chem. Phys. **79**, 2881 (1983).
[21] Y. Seno, N. Kameda, and J. Otsuka, J. Chem. Phys. **72**, 6048 (1980).
[22] J. E. Newton and M. B. Hall, Inorg. Chem.**23**, 4627 (1984).
[23] T. Nozawa, M. Hatano, U. Nagashima, S. Obara, and H. Kashiwagi, Bull. Chem. Soc. Japan **56**, 1721 (1983).
[24] S. Yamamoto and H. Kashiwagi, Chem. Phys. Lett. **161**, 85 (1989).
[25] S. Yamamoto and H. Kashiwagi, Chem. Phys. Lett. **205**, 306 (1993).
[26] J. Bertran, M. F. Ruiz-López, and D. Rinaldi, J. Mol. Str. Theochem. **232**, 337 (1991).
[27] B. H. Huynh, D. A. Case, and M. Karplus, J. Amer. Chem. Soc. **99**, 6103 (1977).
[28] D. A. Case, B. H. Huynh, and M. Karplus, J. Amer. Chem. Soc. **101**, 4433 (1979).
[29] J. Antony, M. Grodzicki, and A. X. Trautwein, J. Phys. Chem. A **101**, 2692 (1997).
[30] C. Rovira, P. Ballone, and M. Parrinello, Chem. Phys. Lett. **271**, 247 (1997).
[31] Y. Tokita and H. Nakatsuji, J. Phys. Chem. B **101**, 3281 (1997).
[32] I. Bytheway and M. B. Hall, Chem. Rev. **94**, 639 (1994).
[33] H. Eicher, D. Bade, and F. Parak, J. Chem. Phys. **64**, 14 (1976).
[34] H. Eicher, F. Parak, D. Bade, and J. Tejada, J. Physique C6 **35**, 363 (1974).
[35] D. Bade and F. Parak, Biophys. Struct. Mechanism **2**, 219 (1976).
[36] F. Parak and G. M. Kalvius, in: Biophysics, W. Hoppe, W. Lohmann, H. Markl, and H. Ziegler (eds.), Springer Verlag, Berlin, Heidelberg, New York 1982.
[37] M. F. Perutz, G. Fermi, B. Luisi, B. Shannan, B, and R.C. Liddington, Acc. Chem. Res. **20**, 309 (1987).
[38] R. Hoffmann, J. Chem. Phys. **39**, 1397 (1963).
[39] T. A. Albright, J. K. Burdett, M. H. Whangbo, Orbital Interactions in Chemistry, J. Wiley & Sons, New York 1985.
[40] C. Kollmar, Int. J. Quant. Chem. **62**, 617 (1997).
[41] M.C. Böhm and R. Gleiter, Theor. Chim. Acta **59**, 127 (1981).
[42] S. Martinez-Carrera, Acta Cryst. **20**, 783 (1966).
[43] J. Kuriyan, S. Wilz, M. Karplus, and G.A. Petsko, J. Mol. Biol. **192**, 133 (1986).
[44] ref. [39], Chapt. 3.
[45] M. C. Böhm, R. D. Ernst, R. Gleiter, and D. R. Wilson, Inorg. Chem. **22**, 3815 (1983).
[46] G. Braunitzer, G. Buse and K. Gersonde, in: Molecular Oxygen in Biology, O. Hayaishi (ed.), Chapt. 6, p. 183, North Holland Publ., Amsterdam 1974.
[47] R. H. Summerville and R. Hoffmann, J. Amer. Chem. Soc. **98**, 7240 (1976).
[48] R. S. Mulliken, J. Chim. Phys. **46**, 497, 675 (1949).